Experimental Neurology 247 (2013) 744–747

Contents lists available at SciVerse ScienceDirect

Experimental Neurology

journal homepage: www.elsevier.com/locate/yexnr

Brief Communication

Neuromyelitis optica-like pathology is dependent on type I interferon response

Reza Khorooshi [a], Agnieszka Wlodarczyk [a], Nasrin Asgari [a,b], Trevor Owens [a,*]

[a] Neurobiology, Institute of Molecular Medicine, University of Southern Denmark, Denmark
[b] Department of Neurology, Vejle Hospital, Denmark

ARTICLE INFO

Article history:
Received 8 January 2013
Revised 2 February 2013
Accepted 8 February 2013
Available online 20 February 2013

Keywords:
Neuromyelitis optica
Type I IFN
Aquaporin-4
Astrocytes
Inflammation

ABSTRACT

Neuromyelitis optica is an antibody-mediated autoimmune inflammatory disease of the central nervous system. Reports have suggested that interferon beta which is beneficial for multiple sclerosis, exacerbates neuromyelitis optica. Our aim was to determine whether type I interferon plays a role in the formation of neuromyelitis optica lesions. Immunoglobulin G from a neuromyelitis optica patient was injected intracerebrally with human complement to type I interferon receptor deficient and wildtype mice. Loss of aquaporin-4 and glial fibrillary acidic protein was reduced in type I interferon receptor deficient mice brain. Our findings suggest that type I interferon signaling contributes to neuromyelitis optica pathogenesis.

Introduction

Neuromyelitis optica (NMO_1) and multiple sclerosis (MS) are inflammatory demyelinating diseases of the central nervous system (CNS) (Lennon et al., 2005). Unlike MS, NMO involves antibodies directed against the water channel aquaporin-4 (AQP4), expressed by astrocytes (Asgari et al., 2011).

Immunoglobulin G (IgG) anti-AQP4 antibody (NMO-IgG) is a serum biomarker for NMO, and evidence from animal models points to a pathogenic role (Asgari et al., 2011, 2013). Interferon beta (IFN-β), a member of the type I IFN family, is an established therapy for relapsing–remitting MS. In contrast, IFN-β appears to be ineffective for preventing NMO relapse and may even increase the relapse rate (Kim et al., 2012; Palace et al., 2010; Tanaka et al., 2009). Such differences in therapeutic response likely reflect differences between the biological disease mechanisms of NMO and MS.

Type I IFNs are cytokines that in addition to their antiviral immune response, exert a regulatory function in inflammatory processes (Benveniste and Qin, 2007). They are produced within CNS by glial cells in response to inflammation or injury (Delhaye et al., 2006; Kallfass et al., 2012; Khorooshi and Owens, 2010; Ousman et al., 2005). Therapeutic action of IFN-β in MS reflects immunomodulatory effects (Benveniste and Qin, 2007). Mice deficient in IFN-β or the common type I IFN receptor (IFNAR) signaling develop severe experimental autoimmune encephalomyelitis (EAE), a model for MS (Prinz et al., 2008; Teige et al., 2003). The role of type I IFN signaling in NMO is unknown.

The goal of the present study was to investigate the role of type I IFN signaling in the formation of NMO-like lesions in brains of mice receiving IgG from a NMO patient and human complement. Intracerebral injection produced characteristic histological features of NMO in brain. There was remarkably reduced AQP4 and glial fibrillary acidic protein (GFAP) loss in the brain of IFNAR-deficient mice compared to wildtype controls. Findings are consistent with a direct effect of type I IFN signaling in NMO pathogenesis, which would explain failure of IFN-β therapy in NMO.

Materials and methods

Mice

Adult female IFNAR-KO on C57BL/6 background were bred from mice originally provided by Dr. Marco Prinz (Prinz et al., 2008). Wildtype (C57BL/6) mice, NMO-IgG and control preparations were as described previously (Asgari et al., 2013).

Intracerebral injections

Stereotactic coordinates were 2 mm lateral from bregma and 0.2 mm anterior. A 30-gauge needle attached to a 50 μl Hamilton syringe was inserted 3.5 mm in the right side of the brain to infuse a total of 10 μl (6 μl NMO-IgG + 4 μl huC′, normal-IgG + huC′ or PBS). The use of

Abbreviations: AQP4, aquaporin-4; C′, complement; CNS, central nervous system; EAE, experimental autoimmune encephalomyelitis; GFAP, glial fibrillary acidic protein; H&E, hematoxylin and eosin; IFNAR, IFN alpha/beta receptor; LFB, luxol fast blue; MS, multiple sclerosis; NMO, neuromyelitis optica.

* Corresponding author at: Neurobiology, Institute of Molecular Medicine, University of Southern Denmark, JB Winsloewsvej 25, 5000 Odense C, Denmark. Fax: +45 6550 3950.
E-mail address: towens@health.sdu.dk (T. Owens).

0014-4886/$ – see front matter © 2013 Elsevier Inc. All rights reserved.
http://dx.doi.org/10.1016/j.expneurol.2013.02.005

human material was approved by the Committee on Biomedical Research Ethics for the Region of Southern Denmark (ref. no. S20080142) and the Danish Data Protection Agency (ref. no. 2008-41-2826). Anesthesia and analgesia were as previously described (Asgari et al., 2013), Danish Ministry of Food, Agriculture and Fisheries ethical approval no. 2012-15-2934-00110. Mice were sacrificed at 2 and 4 days, and brains were dissected out and processed as described previously (Asgari et al., 2013).

Tissue processing and immunostaining

Brain sections were immunostained with primary rabbit antibodies (anti-AQP4 (Alomone Labs Ltd. Jerusalem, Israel), anti-GFAP (DAKO, Denmark), anti-human IgG (Abcam, Cambridge, UK), anti-C5b-9 (C9neo) (Abcam)), anti Iba1 (Wako, Japan), and with secondary biotinylated goat anti-rabbit IgG (Abcam) antibody (Asgari et al., 2013). Specificity of staining was verified as described previously (Asgari et al., 2013). Luxol fast blue (LFB) and hematoxylin and eosin (H&E) staining were used for demyelination and cellular infiltration, respectively. Infiltration and tissue viability were evaluated by H&E staining, and sections showing signs of necrosis related to needle damage were discarded.

Evaluation of histological changes was performed as previously described (Asgari et al., 2013). Based on 4–5 sections for each mouse, pathology was classified with regard to intensity and extent of lesions, whether by staining or loss of staining. Histological changes were graded as: + denotes mild changes of limited extent, ++ denotes moderate changes both by staining intensity or loss and cumulative area and +++ denotes marked changes either very strong staining or total loss of staining over an extensive cumulative area. Results were analyzed by two-tailed unpaired *t*-test using GraphPad Prism software (GraphPad Software Inc., San Diego, California, USA). A p value <0.05 was considered to be statistically significant. Data are presented as mean ± SEM.

Images were acquired using an Olympus DP71 digital camera mounted on an Olympus BX51 microscope (Olympus, Ballerup, Denmark). Images were combined using Adobe Photoshop CS version 10.0.

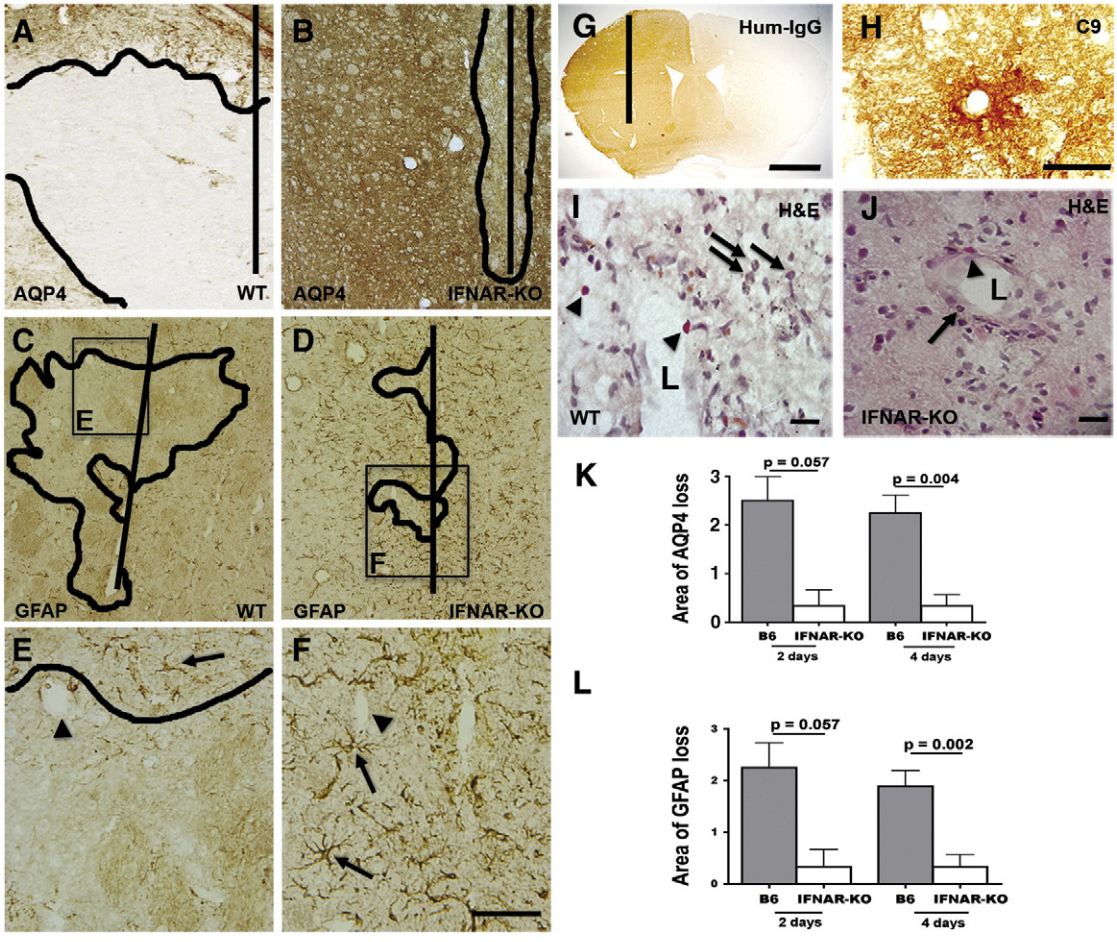

Fig. 1. The loss of AQP4 and GFAP induced by Intracerebral co-injection of NMO-IgG with huC′ was markedly less pronounced in IFNAR deficient than in wildtype mice. A) Injection of NMO-IgG with huC′ into WT mice produced extensive loss of AQP4 in brain parenchyma at 4 days (outlined area) (corresponds to severity: +++) next to the needle track (black line). B) The loss of AQP4 in brain parenchyma (outlined area) (corresponds to severity: +) induced by injection of NMO-IgG with huC′ into IFNAR-KO mice was notably less extensive (black line shows needle track). C) A representative brain section from a WT mouse stained with GFAP showing NMO-IgG + huC′ induced loss of GFAP staining in brain parenchyma (outlined area) (corresponds to severity: +++) next to the needle track (black line), that was notably less pronounced in IFNAR-KO mice (corresponds to severity: +) (D). E) Magnified image of area outlined by box in C (marked E) shows a reactive astrocyte (arrow) outside the affected area (black line) compared to loss of GFAP staining within the affected parenchyma and around a vessel (arrowhead), next to the needle track. F) Magnified image of area outlined by a black box in D (marked F) showing reactive astrocytes (arrows) and a vessel that lacked GFAP staining (arrowhead). G) A representative brain section showing immunoreactivity for human IgG in the injected hemisphere. H) A representative brain section showing C9 immunostaining for deposition of activated complement around a vessel. I–J) Hematoxylin and eosin staining showing infiltrating cells including neutrophils (arrows) and eosinophils (arrowhead) around blood vessels in WT mice (I) and in IFNAR-KO mice (J). At 2 days, the comparison of the area of AQP4 immunostaining loss (K) and GFAP immunoreactivity loss (L) showed no significant differences between wildtype ($n=4$) and IFNAR-KO mice ($n=3$), but at 4 days, it is shown that IFNAR deficiency ($n=9$) resulted in a significant reduction of (K) AQP4 loss at 4 days compared to wildtype mice ($n=8$). L) At 4 days post intracerebral injection, there was a significant loss of GFAP staining in the brain of IFNAR deficient mice ($n=9$) compared to WT ($n=9$). L = lumen. Scale bar in F, 200 μm (A–D) and 100 μm (E–F). Scale bar 1 mm (G), 50 μm (H) 20 μm (I–J).